



# Energy model for contrast detection: spatial-frequency and orientation selectivity in grating summation

Velitchko Manahilov \*, William A. Simpson

*Department of Vision Sciences, Glasgow Caledonian University, City Campus, Cowcaddens Road, Glasgow, G4 0BA, Scotland, UK*

Received 8 August 1999; received in revised form 21 July 2000

---

## Abstract

Models of spatial vision usually assume a ‘front-end’ of spatial-frequency and orientation selective channels. Subthreshold-summation studies have provided some of the strongest support for this notion. We applied a single-channel energy model and a multiple-channels probability-summation model to explore subthreshold-summation phenomena. We measured the contrast thresholds for detection of two superimposed Gabor patches as a function of the spatial-frequency and orientation difference between the components. The stimuli were centred 7.5 deg above the fixation point and were windowed by a Gaussian function with one of two different spatial spreads. We have shown that the spatial-frequency and orientation selectivity in subthreshold summation of Gabor patches is determined by the similarity (cross-correlation) between the stimulus components. A single-channel energy model as well as a multiple-channels probability-summation model could explain the summation data. © 2001 Elsevier Science Ltd. All rights reserved.

*Keywords:* Energy model; Multiple-channels model; Orientation selectivity; Spatial-frequency selectivity; Subthreshold summation

---

## 1. Introduction

Traditional theories of spatial vision generally suppose that early visual processes are served by multiple spatial-frequency and orientation band-pass filters (channels), each sensitive to a restricted range of spatial frequency and orientation (Campbell & Kulikowski, 1966; Campbell & Robson, 1964, 1968). This assumption has been supported by studies on summation of subthreshold gratings (Graham & Nachmias, 1971; Graham & Robson, 1987; Graham, Robson, & Nachmias, 1978; Phillips & Wilson, 1984; Quick, Mullins, & Reichert, 1978; Sach, Nachmias, & Robson, 1971; Watson, 1982). These studies have shown that compound stimuli (consisting of two sinusoidal gratings with the same orientation and spatial frequencies  $F$  and  $3F$  or two gratings with the same spatial frequency whose orientation difference is more

than  $10^\circ$ – $20^\circ$ ) are only slightly more detectable than the components presented alone. Summation between two gratings has been observed when the components are close in spatial frequency and orientation. These selective effects have been described by probability summation among spatially distributed channels which are sensitive to different narrow bands of spatial frequency and orientation at each retinal location.

An energy model for contrast detection (Manahilov & Simpson, 1999a) suggests an alternative explanation of the subthreshold-summation phenomena. According to this model, the cross-correlation between the stimulus components might determine the spatial-frequency and orientation selectivity in grating summation. In the experiments to be reported, we sought to determine whether the cross-correlation between the components in a threshold stimulus might be a reliable predictor of the spatial selective effects. To this end, we studied the summation between two subthreshold Gabor patches as a function of the spatial frequency and orientation difference between the components. The effect of spatial spread of both components on subthreshold summation was also studied.

---

\* Corresponding author.

*E-mail address:* vma@gcal.ac.uk (V. Manahilov).

## 2. Methods

### 2.1. Stimuli

The stimuli were generated with a Pentium computer and displayed on a monitor with 256 grey levels and 12 bits luminance resolution using a method described previously (Pelli & Zhang, 1991). The screen with a mean luminance of 30 cd/m<sup>2</sup> was surrounded by a large screen (100 × 100 cm) illuminated so as to approximate the display in luminance and hue. The stimuli were centred 7.5 deg above the fixation point. Each stimulus consisted of two superimposed components: a vertical grating of spatial frequency ( $v_a$ ) of 6.1 c/deg and a grating of variable spatial frequency ( $v_b$ ) and orientation from vertical ( $\Omega$ ). The sum of the two sinusoidal components was windowed by a two-dimensional Gaussian function. In each stimulus, the contrast ( $f$ ) at a point ( $x, y$ ) is specified by

$$f(x, y) = [Af_a(x, y) + Bf_b(x, y)] \exp[-(x^2 + y^2)/s^2], \quad (1)$$

where:  $f_a(x, y) = \sin(2\pi v_a x + \theta)$  and  $f_b(x, y) = \sin[2\pi v_b(x \cos(\Omega) + y \sin(\Omega))]$  represent unit-amplitude waveform of both components;  $A$  and  $B$  denote the maximal contrast of component  $f_a$  and  $f_b$ , respectively. The component  $f_a$  was presented in two phases ( $\theta$ )—0 and 180°. The spatial constant ( $s$ ) of the Gaussian function was 45' or 22.5'.

In Experiment 1, the monitor had a frame frequency of 75 Hz and the stimulus duration was 27 ms. In Experiment 2, the stimulus components were presented in alternative frames at a rate of 160 Hz (80 Hz for complete image) and the stimulus duration was 50 ms.

### 2.2. Procedure

In Experiment 1, contrast thresholds for stimulus detection were measured by an adaptive Yes/No staircase technique (Watson, 1979; Manahilov & Simpson, 1999a). Initially, three staircases for component  $f_a$  presented alone in phase 0 and 180° and component  $f_b$  presented alone were run simultaneously and randomly. These preliminary data were used to determine the ratios of the contrasts of the components in the compound stimulus. The contrast ratios, thus determined, were kept constant in the main experiment in which nine staircases for nine component combinations were run simultaneously and randomly. Every trial began when the subject pressed an appropriate button and after 500 ms the stimulus was displayed. Two buttons enabled subjects to answer with 'Yes' or 'No' in a period of 5 s. If the subject had blinked, moved his/her eyes or was distracted from the stimuli in any way he/she was able to reject the presented stimulus by not pressing a button. Subjects skipped a trial very rarely, in less than 0.5% of the total trials. We used this option

because subjects felt more comfortable if they knew that some events during stimulus presentation, like eye blinking or eye movements, could not influence task performance. The computer recorded the button press and automatically adjusted the step size for the particular stimulus combination and staircase. Following each 'Yes' response the contrast of the stimulus was reduced and following each 'No' response it was increased by one step. If the current response was identical to the previous one for the stimulus combination and the staircase, the step size was left unchanged. However, if the current response was opposite to the last one, then the step size was twice decreased. This process started at suprathreshold contrast levels with a contrast step of 0.2 log units and continued until the step size became 0.05 log units, after that remaining constant. The subsequent eight reversals for each staircase were used to calculate the contrast threshold for detection of the corresponding component combination. Catch trials (blank stimuli) with a probability of 0.2 were presented. Auditory feedback followed each 'false alarm'. In all experiments only 3% 'false alarms' were given. The responses of the catch trials did not affect the progress of the staircases and were not used in the threshold calculations. Detection thresholds for each experimental condition were measured in four experimental sessions.

In Experiment 2, contrast thresholds were measured using two-interval forced-choice procedure. In preliminary sessions, the contrast thresholds for detection of three components alone (vertical 6-c/deg Gabor patch, vertical 2-c/deg Gabor patch and 6-c/deg Gabor patch tilted 45° to the right of vertical) were measured. To this end we used an adaptive staircase procedure converging to 79% correct responses. In the main experiment, psychometric functions were obtained for the three components presented alone as well as for two complex patterns having far-apart spatial frequencies (vertical Gabor patches of 2 and 6 /deg) and orientations (6-c/deg Gabor patches of vertical orientation and tilted 45° to the right of vertical). Sixty presentations were made at each of five contrasts spaced 0.1 log units apart for the five stimuli which were presented simultaneously and randomly. These ratios of the contrasts of the components were fixed at the estimates of the ratio of their thresholds obtained in the preliminary sessions. Each trial was a two-interval forced-choice trial similar to those of the staircase procedures. The intervals were separated by 500 ms. Each interval was marked by an auditory tone. A feedback tone indicated to the subject if he was incorrect. Two buttons enabled subjects to answer with 'Stimulus was presented during the first interval' or 'Stimulus was presented during the second interval'. Every 4 min a 30-s pause was given in order to decrease sensitivity drift due to fatigue. Each subject took part in four experimental sessions.

2.3. Subjects

One of the authors (VM) and three naive subjects took part in the experiments. Data were collected from two subjects in Experiment 1 and from three subjects in Experiment 2. They viewed the stimulation field binocularly through the natural pupil.

3. Results

3.1. Experiment 1: summation of close spatial frequencies and orientations

In this Experiment we studied summation between a vertical Gabor patch of 6 c/deg and a Gabor patch of variable spatial frequency or orientation from vertical. Fig. 1 shows the relative contrasts for detection of a stimulus ( $s = 45'$ ) at different ratios of the component contrasts. The horizontal and vertical axes indicate the contrast of the components  $f_a$  and  $f_b$ , respectively, in relative units (as described below). When the spatial-frequency or orientation differences between the components were small, the data points fell on an ellipse tilted to the left of vertical (first and second columns in Fig. 1). For larger spatial-frequency or orientation differences, the threshold contrasts formed a nearly circular pattern (right panels in Fig. 1).

3.1.1. Energy model predictions

The data were analysed by an energy model for contrast detection (Manahilov & Simpson, 1999a). This model has three main stages. A single spatiotemporal linear filter transforms the retinal image into a neural representation. It is followed by an energy device which calculates the energy of the neural response ( $E_r$ ) by integrating the squared response ( $g$ ) over space and time within some epoch ( $\theta$ ).

$$E_r = \int_{-\infty}^{+\infty} \int_{-\infty}^{+\infty} \int_0^\theta [g(x,y,t)]^2 dx dy dt. \tag{2}$$

Previous studies have shown that the temporal integration epoch is within the range of 0.2–0.5 s (Koenderink & van Doorn, 1978; Manahilov & Simpson, 1999a; Rashbass, 1970). In the present study we used stimuli of short duration assuming that the duration of the responses to these stimuli is within the range of the estimated values of the temporal integration epoch.

A threshold device signals the presence of the stimulus when the response energy reaches or exceeds a fixed criterion level. Noise is added to the filter output to represent the uncertainty of the detection process. We assume the intrinsic-noise distribution is such that the probability of stimulus detection ( $P$ ) could be approximated by a Weibull function of the response energy.

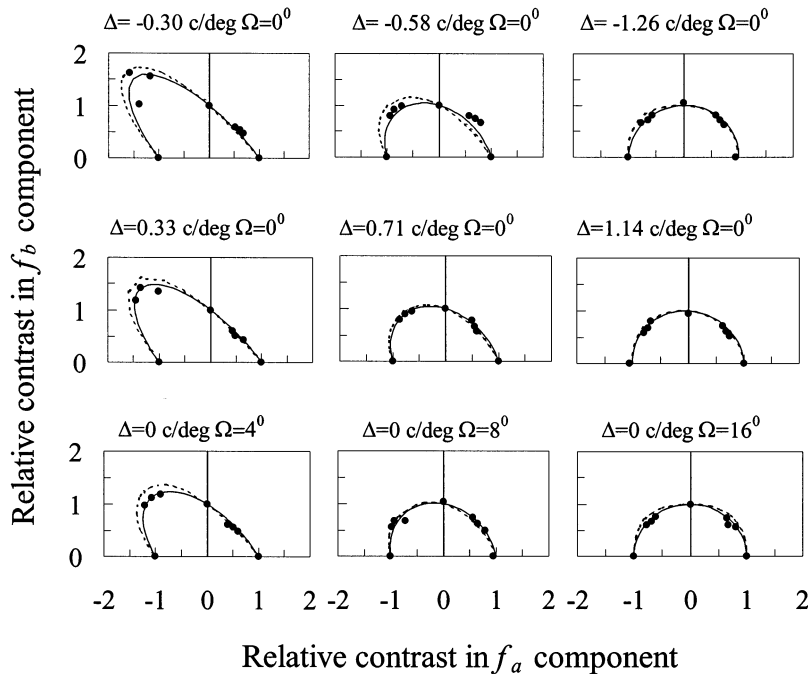


Fig. 1. Plots of relative threshold contrasts in the components of a compound stimulus with  $45'$  spatial spread. Horizontal and vertical axes are expressed in units of the parameters  $\lambda_a$  and  $\lambda_b$ , respectively, obtained by fitting the threshold data with Eq. (4) as described in the text. The thresholds for peaks-subtract (phase  $0^\circ$  in component  $f_a$ ) and peaks-add patterns (phase  $180^\circ$  in component  $f_a$ ) are presented in the first and second quadrant, respectively. Component  $f_a$  is a vertical 6.1-c/deg Gabor patch. The difference between the spatial frequencies of the components ( $\Delta = v_b - v_a$ ) and the difference in orientation from vertical of the component  $f_b$  ( $\Omega$ ) are shown on the top of each graph. The solid curves are best-fitting ellipses to the data points. The dashed curves are predictions from the multiple-channels model. The data are from subject M.M. obtained in individual runs. Standard deviations of the data points are about 0.05 log units.

$$P = 1 - (1 - \gamma) \exp(-E_r^\eta), \quad (3)$$

where  $\eta$  is a constant and  $\gamma$  is the probability of guessing.

At some fixed probability of detection, the spatiotemporal energy of the stimulus response is a constant. The energy model predicts that the threshold contrasts ( $A$  and  $B$ ) of the components of a compound pattern will be given by the equation of an ellipse (see Appendix A):

$$A^2/\lambda_a^2 + B^2/\lambda_b^2 + 2ABK/\lambda_a\lambda_b = 1, \quad (4)$$

where  $\lambda_a$  and  $\lambda_b$  are the threshold contrast for each component when presented alone, and  $K$  is the normalised cross-correlation [Eq. (A6)] between the responses to the components having a unit-amplitude.

It should be noted that previous studies (Manahilov & Simpson, 1999a; Rashbass, 1970; Simpson, 1994; Watson & Nachmias, 1977) considered only one normalisation variable ( $\lambda$ ) because they studied temporal and spatial summation of two identical impulse components and evaluated the auto-correlation function of the impulse response. Here we explored summation of gratings that differed in spatial frequencies or orientation and the threshold contrast for each component when presented alone could be different.

Each set of data was fitted by Eq. (4) with free parameters:  $K$ ,  $\lambda_a$  and  $\lambda_b$ . The solid curves in Fig. 1 illustrate the model predictions calculated with the best-fitting values of the free parameters. The threshold contrasts of the components of each stimulus in Fig. 1 are represented in units of the corresponding  $\lambda_a$  and  $\lambda_b$ . The means of four estimations of the cross-correlation coefficient are presented in Fig. 2 as a function of spatial-frequency (Fig. 2A) and orientation (Fig. 2B) difference between the components. The circles and squares in Fig. 2 represent data from the two subjects tested. The open and filled symbols correspond to data obtained with a stimulus of Gaussian spread of 22.5' and 45', respectively.

These data were compared with the energy model predictions [Eq. (A6)]. The transfer function of the linear filter in one dimension for each subject was constructed by linear interpolation between contrast sensitivity (in a linear-frequency, log-gain sample space) measured for simple Gabor patches of varying spatial frequency (Fig. 3). In two dimensions, the filter was obtained as a surface of revolution of the one-dimensional filter. The predicted cross-correlation coefficients by means of Eq. (A6) (Fig. 2A and B, curves) were in agreement with the cross-correlation coefficients estimated from the summation data using Eq. (4).

Fig. 4 shows the mean values of relative sensitivity for the two subjects (circles — VM and squares — MM) and 95% confidence interval for the data points for subject MM. The relative sensitivity was defined as the reciprocal of the relative contrast threshold for

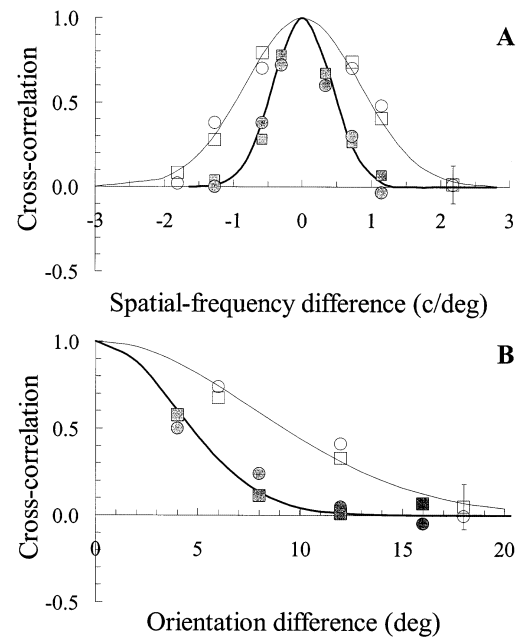


Fig. 2. Cross-correlation between the responses to the components in a compound stimulus. Panel A shows correlation coefficients as a function of the spatial-frequency difference between vertical gratings. Panel B represents correlation coefficients as a function of the orientation difference between 6.1-c/deg components. Empty symbols denote data points obtained with stimuli of 22.5' spatial spread; filled symbols — with stimuli of 45' spatial spread. Squares denote data from subject MM; circles — from subject VM. The data points are estimated by fitting the threshold contours with Eq. (4). The vertical bars represent a typical 95% confidence interval. Thick and thin curves show the energy-model predictions by Eq. (A6) for stimuli of 45' and 22.5' spatial spread, respectively.

detection of component  $f_a$  (or component  $f_b$ ) in a compound stimulus with both components of equal relative contrasts. These sensitivity functions exhibit narrow spatial-frequency and orientation tuning and their bandwidth increases as the spatial spread of the Gabor patches decreases. The solid curves represent the energy-model predictions [Eq. (4)] of the relative sensitivity to stimuli having spatial spread of 45' (thick solid curve) and 22.5' (thin solid curve). The model predictions account satisfactorily for the data points within the experimental errors.

The cross-correlation coefficient captures the similarity between the responses to the stimulus components. Therefore, a given value of the cross-correlation coefficient may be obtained by different combinations of the spatial frequency and orientation of each component and their spatial spread. Fig. 5 presents the relationship between the relative sensitivity and the cross-correlation coefficient for different combinations of the stimulus components. For both subjects we have found that this relationship is strong (the coefficient of correlation was 0.95 for V.M. and 0.98 for M.M.).

3.1.2. Probability-summation model predictions

We also compared the data obtained with the predictions of a probability-summation multiple-channels model as described in Appendix B. According to Eq. (A12), we have the following expression for threshold contrasts  $A$  and  $B$  of stimulus components  $f_a$  and  $f_b$ :

$$\sum_{i=1}^N \iint_{-\infty}^{+\infty} [Af_a(x,y) + Bf_b(x,y)] * h_i(x,y)^\beta dx dy = L. \tag{5}$$

The exponent  $\beta$  describes the steepness of the psychometric function which has been taken to be 3.5, consistent with the psychometric functions collected in other studies (Watson, 1979, 1982; Graham & Robson, 1987). The estimates of half-amplitude bandwidth of the spatial channels are within the range of 0.5–1.5 octaves (Graham, 1989). We performed model calculations assuming that the channels have spatial-frequency bandwidth: (1) 0.5 octaves (spatial spread of 1.5 periods of the carrier; orientation bandwidth of 13°), (2) 1 octave (spatial spread of 0.8 periods of the carrier; orientation bandwidth of 20°); and (3) 1.5 octaves (spatial spread of 0.56 periods of the carrier; orientation bandwidth of 26°). The frequency- and orientation-sampling intervals were one half the frequency and orientation bandwidth, respectively. Only channels whose impulse functions overlap the stimulus in spatial frequency and orientation were considered, because the other possible selective channels are not sensitive to the stimuli used. In the present study the stimuli were presented 7.5 deg above the fixation point, where contrast sensitivity at different positions in the visual field is approximately constant (Robson & Graham, 1981). That is why the sensitivity of each channel across the visual field was constant. This model was used to

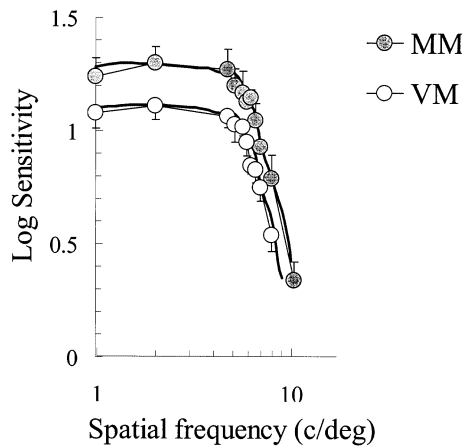


Fig. 3. Contrast sensitivity functions for two subjects. The stimuli are Gabor patches centred 7.5 deg above the fixation point. Stimulus spatial spread is 45'. The vertical bars represent 95% confidence intervals. Thin lines were constructed by linear interpolation between sample values. Thick curves represent predictions by the probability-summation model as described in the text.

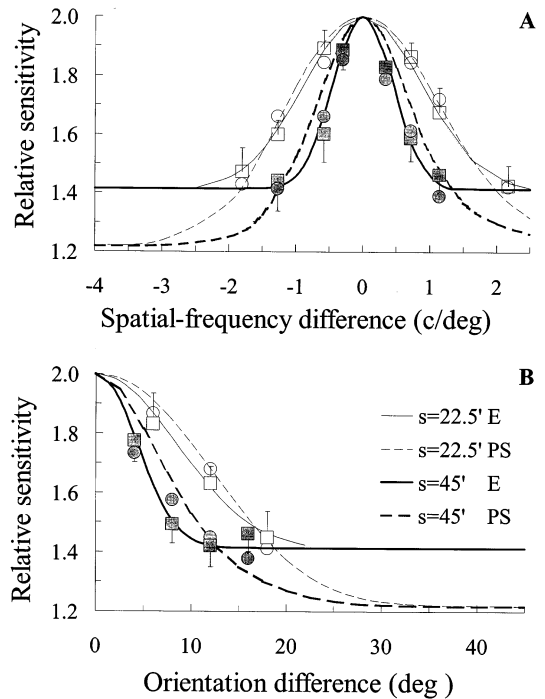


Fig. 4. Relative sensitivity in compound stimuli with both components of equal relative contrast defined as the reciprocal of the relative contrast threshold for detection of component  $f_a$  (or component  $f_b$ ). Panel A shows relative sensitivity as a function of the spatial-frequency difference between vertical components. Panel B illustrates relative sensitivity as a function of the orientation difference between 6.1-c/deg components. Thick curves show model predictions for stimuli of 45' spatial spread, thin curves represent model predictions for stimuli of 22.5' spatial spread. Solid curves are calculated by the energy model, dashed curves are computed by the probability-summation model assuming that channel bandwidth is 0.5 octave and  $\beta = 3.5$ . The vertical bars represent the 95% confidence interval for subject MM which is similar to the 95% confidence interval for the other subject. The other designations are as in Fig. 2.

compute relative threshold contrasts in the components of a compound stimulus. However, the sensitivity of each channel can influence summation predictions (Quick, Mullins, & Reichter, 1978). The sensitivity of each channel ( $c_i$ ) has been adjusted so that the model approximately predicts the thresholds for detection of Gabor patches presented alone (thick curves in Fig. 3).

The thin curves in Fig. 6 show the relative sensitivity predicted by probability- summation model. As the channel frequency bandwidth decreases, the sensitivity function becomes narrower (Fig. 6A). These predictions are in line with model calculations in the spatial-frequency domain, reported by Quick, Mullins, and Reichter (1978) and Watson (1982). A similar relationship was observed in the orientation domain (Fig. 6B). An important characteristic of these functions is that as the separation in spatial frequency and orientation of the components increases the relative sensitivity approaches an asymptote that reflects activation of independent channels and its value at  $\beta = 3.5$  is equal to  $1.21 (2^{1/\beta})$ .

Thus, when  $\beta = 2.5$ , the asymptote is 1.31. Dashed lines in Fig. 6 illustrate predictions of probability-summation model assuming  $\beta = 2.5$  and frequency bandwidth of 0.5 octaves.

The dotted curves in Fig. 1 shows model predictions assuming channels whose bandwidth is 0.5 octaves and  $\beta = 3.5$ . It should be noted that we have not attempted to fit these curves to the data. We found that the predicted threshold contours had an elliptical form when the spatial-frequency or orientation differences between the components were small and a circle-like form for larger spatial-frequency or orientation differences in the components. These predictions were very close to the data obtained.

The dashed curves in Fig. 4A and B show the relative sensitivity predicted by channels having bandwidth of 0.5 octaves and  $\beta = 3.5$ . The model predictions appear to give a good fit to the data. Note that the probability-summation model predicts that the bandwidth of relative-sensitivity functions depends on the spatial spread of the stimulus components.

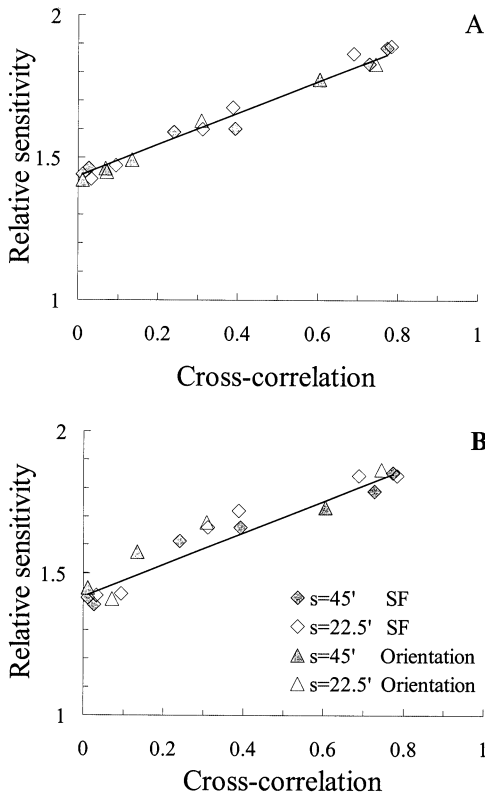


Fig. 5. Relative sensitivity to compound stimuli as a function of the cross-correlation between the stimulus components. The cross-correlation coefficients are calculated for different combinations of component spatial-frequency, orientation and spatial spread. Upper panel shows data from subject MM, bottom panel represents data from subject VM.

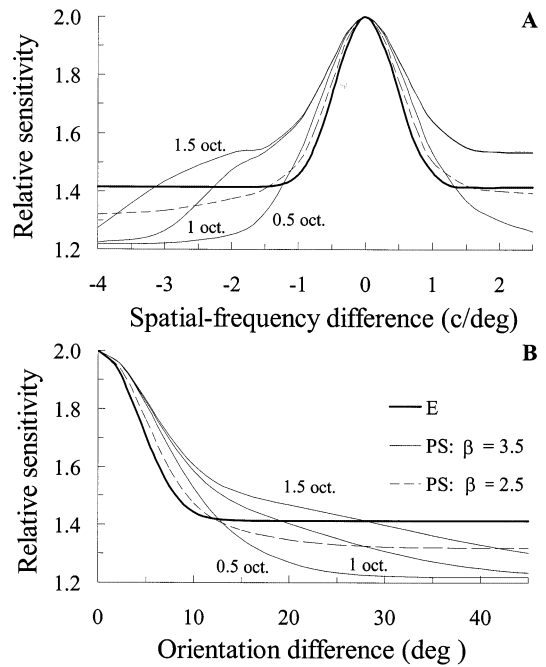


Fig. 6. Calculated relative sensitivity in compound stimuli with both components of equal relative contrast as a function of the spatial-frequency difference between vertical components (panel A) and as a function of the orientation difference between 6.1-c/deg components (panel B). The stimulus spatial spread is 45'. Thick curves represent energy model predictions. Thin solid curves are calculated by the probability-summation model assuming that channel bandwidth is 0.5, 1 and 1.5 octaves and  $[GCU1]\beta = 3.5$ . Thin dashed curves are computed by the probability-summation model assuming that channel bandwidth is 0.5 octaves and  $[GCU2]\beta = 2.5$ .

### 3.1.3. Matched-filter model predictions

Cross-correlation models, also known as matched-filter models, are based on the ideal-observer approach (Burgess & Ghandeharian, 1984; Green & Swets, 1974; Hauske, 1988; Rovamo, Luntinen, & Näsänen, 1993). The cross-correlator has the best performance in a detection task under the assumptions that it knows a priori the signal parameters exactly and the noise in which the signal is embedded is uncorrelated. Such an observer detects the stimulus when the cross-correlation of the expected signal with the presented noise or signal plus noise reaches or exceeds a fixed criterion level. It should be noted that an ideal observer will be an energy detector in some circumstances. When the observers do not have any information about the stimuli, an energy (incoherent) energy algorithm would detect the stimuli most optimally.

Hauske (1988) pointed out that matched-filter models could explain the summation of gratings having close spatial frequencies. In the present study, we consider a mismatched cross-correlation model, which similarly to the probability-summation model, assumes the existence of a limited set of filters ( $h_i$ ) having narrow spatial-frequency bandwidth (Kersten, 1984). The re-

sponse output of the cross-correlator ( $R$ ) is given by the cross-correlation of the stimulus waveform ( $f$ ) and the filter functions ( $h_i$ ):

$$R = \iint_{-\infty}^{+\infty} f(x,y)h_i(x,y)dx dy. \quad (6)$$

Consider a stimulus which consists of two components  $f_a$  and  $f_b$  whose threshold contrasts are  $A$  and  $B$ , respectively. In such a case, Eq. (6) may be written as follows:

$$\begin{aligned} R &= \sum_{i=1}^N \iint_{-\infty}^{+\infty} [Af_a(x,y) + Bf_b(x,y)]h_i(x,y) dx dy \quad (7) \\ &= A \sum_{i=1}^N \iint_{-\infty}^{+\infty} f_a(x,y)h_i(x,y) dx dy \\ &\quad + B \sum_{i=1}^N \iint_{-\infty}^{+\infty} f_b(x,y)h_i(x,y) dx dy. \\ &= \text{const.} \end{aligned}$$

Denoting the threshold contrasts for the two components alone with  $\lambda_a$  and  $\lambda_b$ , Eq. (7) may be expressed as:

$$A/\lambda_a + B/\lambda_b = 1. \quad (8)$$

This model predicts linear summation between the stimulus components, that is the sum of the relative contrasts of the two components is constant and equal to 1.0, regardless of the difference of the components in spatial frequency or orientation. This prediction is in line with summation of gratings having close spatial frequency. Indeed, Fig. 1 shows that threshold contours (in the first quadrant) for gratings of close spatial frequencies and orientations are closer to straight lines than to convex curves. Such a prediction, however, deviates significantly from threshold contours for Gabor patches having larger spatial-frequency or orientation differences.

### 3.2. Experiment 2: summation of far-apart spatial frequencies and orientations

In Experiment 1, we found that the energy model as well as the probability-summation model can account for the data on summation of components having close spatial frequencies and orientations. The predictions of these models differ mainly for components having far-apart spatial frequencies and orientations and we will compare the model fits to data obtained using these stimulus parameters. So far we have assumed that the exponent  $\beta$  has the typical value 3.5. Unfortunately, in Experiment 1 we measured contrast thresholds using a staircase procedure which did not allow estimation of the exponent  $\beta$ . That is why in Experiment 2 we used the method of constant stimuli to study summation of Gabor patches of 45'-spatial spread having far-apart spatial frequencies and orientations. Two complex stim-

uli were used. The first one consisted of vertical Gabor patches of 6 and 2-c/deg. The second one had two components of 6-c/deg: a vertical Gabor patch and a Gabor patch tilted 45° to the right of vertical. Fig. 7 represents the psychometric functions (proportion correct responses as a function of stimulus contrast) measured in one session with subject LE for detection of the vertical 6-c/deg component (panel A), the vertical 2-c/deg component (panel B) and the tilted 6-c/deg component (panel C). The psychometric functions for components presented alone are denoted with filled symbols, those measured in the presence of a second component are denoted by empty symbols. The results presented in Fig. 7 show that the psychometric functions for the components alone are shifted to higher contrast levels and are steeper as compared to components presented in the complex stimulus Fig. 8.

Sixty sets of psychometric functions were individually fitted by the Weibull function:

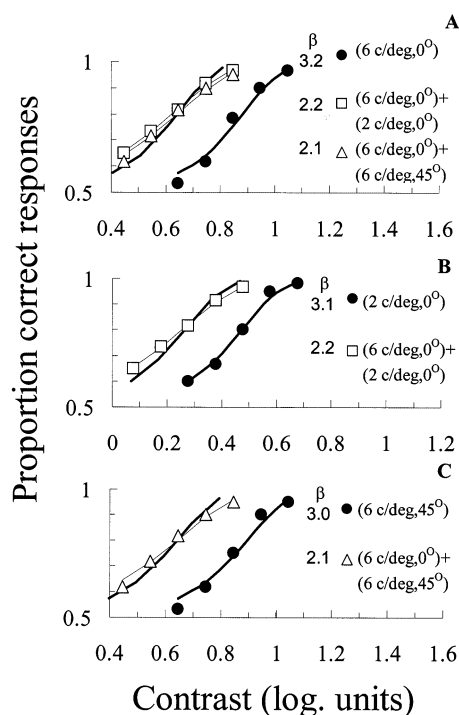


Fig. 7. Psychometric functions defined as proportion correct responses as a function of stimulus contrast. Panel A shows psychometric functions for detection of a vertical 6-c/deg component. Panel B represents psychometric functions for detection of a vertical 2-c/deg component. Panel C illustrates psychometric functions for detection of a tilted 6-c/deg component. Filled symbols show psychometric functions for components presented alone. Empty symbols show psychometric functions for detection of the corresponding component in a complex stimulus. Curves present psychometric functions calculated by [Eq. (10)] having the best fitting parameters (see text for details). Thin curves show psychometric functions for components in a complex stimulus; thick curves — for components alone. The thick curves are shifted in horizontal direction to fit the data for components in a complex stimulus. Estimates of the exponent  $\beta$  are shown in insets. Data for subject LE are shown.

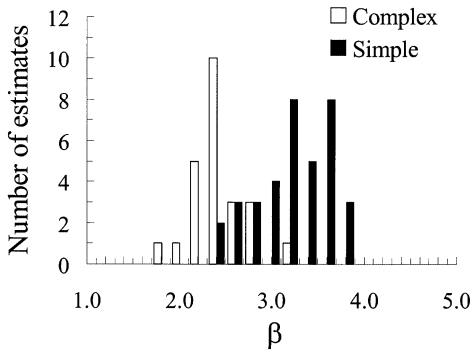


Fig. 8. Distribution of estimates of the exponent  $\beta$ . Empty bars show estimates for complex stimuli having two components. Filled bars illustrate estimates for simple stimuli, that is the components presented alone. Data for three subjects are shown.

$$P = 1 - 0.5 \exp[-C/\alpha]^\beta, \tag{9}$$

where  $P$  is the proportion correct responses,  $C$  is the contrast,  $\beta$  is the slope of the function, and  $\alpha$  is the threshold contrast (the contrast at which  $P = 0.82$ ). We applied the fitting procedure described by Watson (1979), which provides maximum likelihood estimates of  $\beta$  and  $\alpha$ . Fig. 8 illustrates the distribution across the subjects of the number of estimates of the exponent  $\beta$ . We found that the distribution of all estimates of  $\beta$  is broad and bimodal. The empty bars show the distribution of the estimates of  $\beta$  for components in complex stimuli which have a mean of 2.3 and a standard deviation of 0.3. The distribution of the estimates of  $\beta$  for components presented alone is represented by filled bars. These estimates were averaged, yielding a mean of 3.3 and standard deviation of 0.4. The mean value and standard deviation of  $\beta$  obtained with simple and complex stimuli is 2.9 and 0.6, respectively.

We assume that there is no channel sensitive to components having far-apart spatial frequencies or orientations. Thus, at threshold, Eq. (5) could be written as:

$$|A|^\beta / |\lambda_a|^\beta + |B|^\beta / |\lambda_b|^\beta = 1, \tag{10}$$

where:  $A$  and  $B$  denote the contrasts of the two components in a complex stimulus;  $\lambda_a$  and  $\lambda_b$  are the threshold contrast for each component alone. The estimated contrast thresholds for each complex stimulus and the corresponding components alone were fitted by a curve defined by Eq. (10).

We used the approach described by Graham and Robson (1987) to fit the curve calculated by Eq. (10) to the three thresholds from a single run. This fitting procedure allows specifying the free parameters ( $\lambda_a$ ,  $\lambda_b$  and  $\beta$ ) by minimising the sum of distances, described as follows:

$$\sum_{i=1}^3 |(A_i/\lambda_a)^\beta + (B_i/\lambda_b)^\beta - 1|. \tag{11}$$

Fig. 9 shows the results (averaged across experimental sessions) of the three subjects for summation of the vertical 6-c/deg and 2-c/deg components (empty symbols) and for summation of the vertical and tilted 6-c/deg components (filled symbols). The mean value and the standard deviation of the exponent  $\beta$  across the subjects is 2.2 and 0.3, respectively. The curve in Fig. 9 illustrates the threshold contour corresponding to  $\beta = 2.2$ . The relative sensitivity estimated by use of this value of the exponent  $\beta$  is shown in Fig. 10 (black bar). The predictions of the probability-summation model using the exponent  $\beta$  (2.3) estimated from psychometric functions of the components in complex stimuli are illustrated by the bar with horizontal stripes. The bar with vertical stripes denotes the predictions of this model using the exponent  $\beta$  (2.9) obtained with simple and complex stimuli, and the crossed-hatched bar shows the predictions using exponent  $\beta$  (3.3) derived from psychometric functions for simple stimuli. We performed  $t$ -tests and found that the estimated relative sensitivity did not differ at 95% confidence level from those predicted by the energy model (empty bar) and the probability-summation model based on the exponent  $\beta$  obtained with complex stimuli. The other two predictions of the probability-summation model differed significantly at the 95% confidence level from the estimated relative sensitivity.

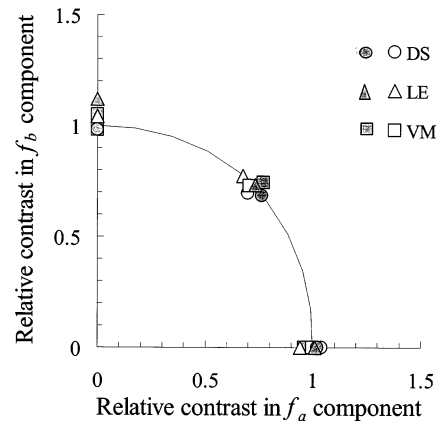


Fig. 9. Relative threshold contrasts in the components of a complex stimulus of 45' spatial spread. Horizontal and vertical axes are expressed in units of the parameters  $\lambda_a$  and  $\lambda_b$ , respectively, obtained by fitting the threshold data with Eq. (10) as described in the text. Empty symbols show relative threshold contrasts of the vertical 6-c/deg component and the vertical 2-c/deg component. Filled symbols illustrate relative threshold contrasts of the vertical 6-c/deg component and the tilted 6-c/deg component. The curve shows the threshold contour calculated by Eq. (10) with  $\beta = 2.2$ . Averaged data for three subjects are shown.

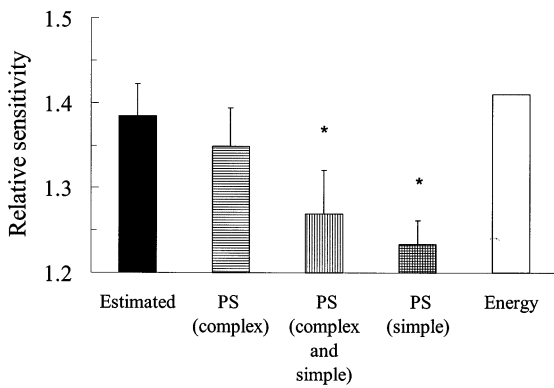


Fig. 10. Relative sensitivity in compound stimuli whose components have equal relative contrasts and far-apart spatial frequencies and orientations. Black bar shows the relative sensitivity estimated by  $\beta = 2.2$  obtained from the summation data. Bar with horizontal stripes illustrates the predictions of the probability-summation model using the exponent  $\beta = 2.3$  estimated from the psychometric functions of the components in complex stimuli. Bar with vertical stripes denotes the predictions of the probability-summation model using the exponent  $\beta = 2.9$  obtained with simple and complex stimuli. Crossed-hatched bar shows the predictions of the probability-summation model using exponent  $\beta = 3.3$  derived from psychometric functions for simple stimuli. Vertical bars — 95% confidence interval. \* above the third and fourth bars indicate that these data are significantly different from the data presented by the first bar. Averaged data for three subjects are shown.

#### 4. Discussion

The present study has confirmed previous findings that subthreshold summation occurs for stimuli having components of closely similar spatial frequencies (Graham & Robson, 1987; Quick, Mullins, & Reichter, 1978; Sach, Nachmias, & Robson, 1971; Watson, 1982) and orientations (Phillips & Wilson, 1984). In addition, we have shown that both spatial-frequency and orientation sensitivity functions are narrower for summation of larger Gabor patches (Fig. 4). This behaviour of subthreshold summation might be explained by the cross-correlation between the responses to the stimulus components in the framework of a single-channel energy model for contrast detection (Manahilov & Simpson, 1999a). We established that the amount of summation between two Gabor patches is proportional to the cross-correlation between the responses to the components, irrespective of the type of the stimulus parameter (spatial frequency or orientation of each component and spatial spread of both components) that determines this coefficient (Fig. 5).

It should be noted that the cross-correlation reflects the similarity between the stimulus components themselves. This is because the contrast sensitivity function in Eq. (A6) could be considered constant in the frequency range where the spectra of the components are nonzero. However, this constant is cancelled due to the normalisation of the cross-correlation coefficients by

the square root of the response energy of the individual components and Eq. (A6) could be boiled down to the normalised cross-correlation between the stimulus components. Therefore, one may conclude that both spatial-frequency and orientation sensitivity functions, estimated by summation of subthreshold gratings, are determined by the degree of similarity between the stimulus components.

Graham (1989) pointed out that the stimulus components in grating summation experiments could differ in seven spatial dimensions: spatial frequency, orientation, spatial position (two dimensions), spatial extent (two dimensions), and spatial phase. Stimulus components could also vary in four temporal dimensions: temporal frequency, temporal position, temporal extent, and temporal phase. Usually in an experiment, the two stimulus components differ only in their value along one (experimental) dimension. The present study was aimed at testing the hypothesis that the cross-correlation between the components in a threshold stimulus might be a reliable predictor of the spatial selective effects. To this end, we studied the summation between two subthreshold Gabor patches as a function of the spatial-frequency and orientation difference between the components having two different spatial spreads. We have chosen these stimulus parameters because a given value of the cross-correlation coefficient may be obtained by different combinations of the spatial frequency and orientation of each component, as well as the spatial spread of the components. If the stimulus components vary in the four temporal dimensions mentioned above, cross-correlation coefficients should be defined in both spatial and temporal domains. Testing these predictions requires additional future studies.

The data obtained were also analysed by a multiple-channels probability-summation model (Graham, 1989; Graham & Robson, 1987; Graham, Robson, & Nachmias, 1978; Watson, 1982). Assuming that the channels have spatial-frequency bandwidth of 0.5 octaves and the steepness of the psychometric functions  $\beta$  is equal to the typical value of 3.5, the model described well the data for small differences in the component spatial frequency and orientation (Experiment 1). This model also predicted the observed effect of the stimulus spatial spread on the tuning of the spatial-frequency and orientation sensitivity functions (Fig. 4). The energy and probability-summation models predict different relative sensitivities for components having far-apart spatial frequencies and orientations (Fig. 6). In Experiment 2 we tested these predictions. Using the method of constant stimuli, we have established that the slope of the psychometric functions significantly depends on the stimuli used. Simple stimuli having a single component exhibit steeper psychometric functions than those for complex stimuli consisting of two components (Fig. 7). This result is not in line with the findings by Graham

(1989) which have shown that the psychometric functions for simple and complex gratings have similar slopes ( $\beta = 4$ ). On the other hand, Nachmias (1981) has found that  $\beta$  estimates are consistently higher by 20–60% for gratings of 12 c/deg than for bipartite fields. The slope of the psychometric function is a crucial parameter for probability-summation models. These models are based on the homogeneity assumption stating that the exponent  $\beta$  of the psychometric function [Eq. (A9)] of each detector at a given location is a constant (Graham, 1989; Nachmias, 1981). In other words, the psychometric functions for different stimuli should have exactly the same shape when plotted against logarithmic contrast. Having in mind the present findings, a question arises of how to apply the Quick pooling concept if the homogeneity assumption is not valid. Fig. 9 illustrates the complexity of this problem: different conclusions could be made using different estimates of the exponent  $\beta$ . We have found a good agreement between the relative sensitivities estimated from the summation data and those predicted by the probability-summation model using the slope of the psychometric functions for the components presented simultaneously. The predictions based on the slope obtained with simple and complex stimuli as well as only with simple stimuli differed significantly from the estimated relative sensitivity. The existence of differences among the slopes of the psychometric functions for different patterns suggests that the model should allow the exponent  $\beta$  to be different for different detectors. This would drastically complicate the model. In addition, the Quick pooling formula [Eq. (9)] is based also on the high-threshold assumption (Graham, 1989; Nachmias, 1981) which states that the internal threshold criterion has been set so high that it is never exceeded on trials of the blank stimulus. However, false alarms do occur and they have been taken into account by incorporating a guessing parameter. If the high-threshold assumption were correct, the probability of correct response in a forced-choice experiment after correction for 'guessing' and the probability of saying 'yes' in a yes–no experiment should give consistent estimates of the observer's probability of detecting the stimulus. There is evidence that this prediction is wrong (Nachmias, 1981). Therefore, the main assumptions underlying the Quick pooling formula seem to be not correct. However, Graham (1989) considered an alternative interpretation of the Quick pooling formula as deterministic non-linear pooling without a necessary relationship between the slope of the psychometric function and the amount of summation.

The differences among the slopes of the psychometric functions for different patterns also raise problems for the energy model as presented in this paper. In this model, the slope of the psychometric function determines the energy of the responses to threshold stimuli

[Eq. (3)] and the relative sensitivity for detection of component  $f_a$  (or component  $f_b$ ) in a compound stimulus depends on the performance level chosen for threshold. For example, let us calculate the relative probability using Eqs. (3) and (4), performance level of 0.70% correct, exponent  $\beta = 2.3$  for components alone and  $\beta = 3.3$  for components in a complex stimulus. Having in mind that when the probability of stimulus detection in Eq. (3) is expressed as a function of stimulus contrast, the exponent  $\eta$  is equal to  $\beta/2$ , we will find that the relative sensitivity is 1.29. This value is about 9% smaller than the predicted value of 1.41 if the homogeneity assumption were correct. However, for a performance level of 0.82, which is the value we used to evaluate the detection threshold from the psychometric functions, the relative sensitivity is 1.41. It should be noted that energy models have been used satisfactorily to describe detection of temporal stimuli (Koenderink & van Doorn, 1978; Manahilov & Simpson, 1999a; Rashbass, 1970; Watson & Nachmias, 1977), spatial summation of elliptical Gaussian blobs (Bijl & Koenderink, 1993), temporal summation of two motion impulses (Simpson, 1994), and pairs of spatially separated line stimuli (Manahilov & Simpson, 1999a). An energy-detector model has been also applied by Hall and Sondhi (1977) to describe auditory data on detection of two-tone signals at different frequency separations between the component frequency. According to signal detection theory (Green & Swets, 1974), the energy algorithm is the most optimal algorithm when the observers do not have any information about the signal being detected. In Experiment 1, nine staircases for nine component combinations were run simultaneously and randomly. In Experiment 2, psychometric functions were obtained simultaneously for the three components presented alone and in two complex patterns. Under these conditions, the subject could apply an energy algorithm in stimulus detection.

Within the framework of signal detection theory, if the observer knows the signal waveform exactly and the signal is embedded in uncorrelated noise, the most optimal detection algorithm is cross-correlation of the expected signal with the presented noise or signal plus noise (Burgess, 1999; Green & Swets, 1974). We considered a mismatched cross-correlation model assuming that the visual system contains a limited set of filters having narrow spatial-frequency bandwidth (Kersten, 1984). This model predicts linear summation between the stimulus components regardless of the difference of the components in spatial frequency or orientation. This prediction differs from the non-linear summation between Gabor patches of different spatial frequency and orientation that was observed in the present and other studies.

The shallower psychometric functions obtained with complex stimuli indicate that detection of these stimuli

is more variable than detection of simple stimuli having steeper psychometric functions. This could be explained by recently published data on dynamics of preferred spatial-frequency and orientation of cells in macaque primary visual cortex obtained by a reverse-correlation approach (Ringach, Hawken, & Shapley, 1997; Ringach, Bredfeldt, Dorn, Spriggs, & Irazoqui-Pastor, 2000). It was found that V1 cells exhibit a shift of their preferred spatial frequency from low to high spatial frequencies as the response develops over time. Similarly, the preferred orientation of V1 cells changes with time. These findings suggest that a single cell could act over time as detector of different spatial frequencies and orientations. Such a detector should detect complex stimuli having two components of far-apart spatial frequencies and orientations over longer period than components alone. This might result in: (1) larger variability of detection of complex stimuli (and shallower psychometric functions) compared to detection of simple stimuli, and (2) higher probability summation over time and lower threshold contrasts for detection of complex stimuli in comparison with those for detection of simple stimuli. The second suggestion could explain the high value of relative sensitivity (1.38) to the components (having far-apart spatial frequencies and orientations) in complex stimuli which was obtained in Experiment 2. The neurophysiological data considered above are related to responses of V1 cells to impulse stimuli. Therefore, the above speculation could be applied to the present study of summation of stimuli having short duration.

It should be noted that studies on summation of subthreshold gratings having far-apart spatial frequencies and orientations (Graham & Nachmias, 1971; Graham & Robson, 1987; Phillips & Wilson, 1984; Quick, Mullins, & Reichert, 1978; Watson, 1982) found that the relative sensitivity is about 1.2. Most of these studies used stimuli whose duration was in the range 200–750 ms. These findings were explained by non-linear summation of stochastically independent channels, each of which is sensitive to only one of the two stimulus components. These channels were considered only in space and the integration epoch of probability summation was assumed to be infinite. Certainly, the dynamics of detector responses should be taken into account. It should be noted that our summation data are also not in line with the data from Experiment 3 by Watson and Nachmias (1980) who used briefly presented stimuli in conditions similar to those of the present experiment. This study established that relative sensitivity to the components of the complex stimulus is about 1.2. On the other hand, Wilson (1980) studied summation between components having 0.25 and 0.75c/deg and

transient temporal presentation (1 cycle of an 8 Hz square-wave). He found more summation between components in peaks-add mode than expected from multiple-channels model. Resolving these discrepancies requires additional studies using stimuli of short duration.

In the present study we tested some algorithms that could explain summation of subthreshold patterns. It should be noted that the ModelFest project (Watson, 2000) was aimed at collection of luminance contrast thresholds for 43 two-dimensional patterns and testing of visual models for contrast detection. The data collected were fitted with three single-channel models (peak contrast, energy and generalised energy) and two multiple-channels models (Gabor channels and discrete cosine transform). The results showed that with the exception of the peak contrast model, the Gabor channels model provided the best fit, and the other models provide remarkably good fits of the experimental data. The author concluded that:

This leads to a further intriguing result. Much of the theoretical and experimental work in spatial vision in the last thirty years has focussed upon spatial channels; on their existence and on their detailed shape and number. However in this exercise, while the Gabor channel model does provide the best fit, it is not much better than a model with rather crude channels (D[iscrete]T[ransform]16), or with no channels at all (G[eneralised]E[nergy]). Thus while channels may be strongly implied by other psychophysical results, their effects here are modest, and evinced mainly by broadband stimuli. (Watson, 2000: 31)

This conclusion is in line with the results of the present study showing that a single-channel energy model as well as a multiple-channels probability-summation model could explain data on summation of Gabor patches. Results have also revealed that the tuning of both spatial-frequency and orientation sensitivity functions reflects the cross-correlation between the stimulus components. It should be noted that Caelli and Moraglia (1987) came to similar conclusions concerning pattern-masking effects. They found that the masking effects of a pattern on a test stimulus can be indexed by the cross-correlation between the stimuli. Therefore, one may suggest that a measure of the similarity between the stimulus components might give valuable constraints for the understanding of spatial vision. In the present experiments we studied subthreshold summation only of Gabor patches. Further studies of summation phenomena with natural images will be used to verify the present suggestions.

**Acknowledgements**

This work was supported in part by Grant I 622 from the National Scientific Research Fund, Bulgarian Ministry of Education, Science and Technology and a Centre of Excellence Grant from the Glasgow Caledonian University to the Department of Vision Sciences (VM). We are grateful to the anonymous referees for the valuable suggestions and comments of the previous version of the manuscript. This work has previously been presented in abstract form (Manahilov & Simpson, 1999b).

**Appendix A**

The predictions of the energy model (Manahilov & Simpson, 1999a) are derived here. In the present study, we used stimuli whose spatial parameters were only varied and we will analyse the response energy only in space domain. Applying the Rayleigh’s and convolution theorems (Bracewell, 1978), the energy of the response [Eq. (2)] to a compound stimulus, having two components of threshold contrasts *A* and *B*, may be written in spatial frequency domain ( $f_x, f_y$ ) as:

$$\int\int_0^\infty [AF_a(f_x, f_y)H(f_x, f_y) + BF_b(f_x, f_y)H(f_x, f_y)]^2 df_x df_y = \text{const} \tag{A1}$$

where  $F_a$  and  $F_b$  are the Fourier transforms of the waveform of a unit-amplitude stimulus  $f_a$  and  $f_b$ , respectively and  $H$  is the spatiotemporal transfer function of the linear filter.

Eq. (A1) may be expressed as follows:

$$\begin{aligned} &A^2 \int\int_0^\infty [F_a(f_x, f_y)H(f_x, f_y)]^2 df_x df_y \\ &+ B^2 \int\int_0^\infty [F_b(f_x, f_y)H(f_x, f_y)]^2 df_x df_y \\ &+ 2AB \int\int_0^\infty [F_a(f_x, f_y)H(f_x, f_y)] \\ &\times [F_b(f_x, f_y)H(f_x, f_y)] df_x df_y = \text{const} \end{aligned} \tag{A2}$$

Defining  $\lambda_a$  and  $\lambda_b$  as the threshold contrasts for  $f_a$  and  $f_b$  components alone, Eq. (A2) may be written as:

$$A^2/\lambda_a^2 + B^2/\lambda_b^2 + 2ABK/\lambda_a\lambda_b = 1, \tag{A3}$$

where  $K$  is the normalised cross-correlation between the responses to the components having a unit-amplitude:

$$K = \frac{\int\int_0^\infty F_a F_b H^2 df_x df_y}{\left[ \int\int_0^\infty (F_a H)^2 df_x df_y \int\int_0^\infty (F_b H)^2 df_x df_y \right]^{1/2}} \tag{A4}$$

We could approximate the transfer function of the visual system by the contrast sensitivity function (CSF). Assuming a radial symmetry of CSF in the  $f_x, f_y$  domain (similar contrast sensitivity functions to gratings of different orientation) we may write

$$|H(f_x, f_y)| = L \text{CSF}(f_x, f_y), \tag{A5}$$

where  $L$  is a constant.

Substituting  $H$  in Eq. (A4), the cross-correlation becomes:

$$K = \frac{\int\int_0^\infty F_a F_b \text{CSF} df_x df_y}{\left[ \int\int_0^\infty (F_a \text{CSF})^2 df_x df_y \int\int_0^\infty (F_b \text{CSF})^2 df_x df_y \right]^{1/2}} \tag{A6}$$

**Appendix B**

The predictions of the probability-summation model (Graham, 1989; Graham, Robson, & Nachmias, 1978; Quick, 1974; Watson, 1979, 1982) are derived here. This model assumes the existence of multiple channels tuned to different bands of spatial frequency. Each channel is a collection of many detectors which respond to a particular band of spatial frequency and are distributed over visual space. An important issue in this model is that channels responding to different bands of spatial frequency serve the same retinal area. The impulse function ( $h$ ) of the detector [at location  $(x_o, y_o)$ ] of channel  $i$  is defined by the product of a two dimensional circular Gaussian function and a sine function of frequency  $v_i$ :

$$\begin{aligned} &h_i(x-x_o, y-y_o) \\ &= c_i \exp[-((x-x_o) - (y-y_o))^2 v_i^2 / s^2] \sin[2\pi v_i(x-x_o)], \end{aligned} \tag{A7}$$

where  $s$  is the spatial spread of the Gaussian, expressed in periods of the detector frequency and  $c_i$  is a factor governing the sensitivity of channel  $i$ .

We assume that uncorrelated noise is added to the response of each detector and when the magnitude of the noisy response exceeds a criterion level, the detector detects the signal. The probability of seeing the stimulus ( $P$ ) may be expressed by the probability of guessing ( $\gamma$ ) and the probability that at least one sample in  $(x, y)$  space of the noisy response ( $P_{i,x,y}$ ) has exceeded the criterion level:

$$P = 1 - (1 - \gamma) \prod_i \prod_x \prod_y (1 - P_{i,x,y}). \tag{A8}$$

The probability that the detector at location  $(x, y)$  will signal the occurrence of a stimulus depends on the magnitude of its response ( $g_i$ ) at that location by the following manner (Quick, 1974):

$$P_{i,x,y} = 1 - \exp(-|g_i(x,y)|^\beta), \quad (\text{A9})$$

where the exponent  $\beta$  describes the steepness of the psychometric function.

Assuming that the detectors of each channel have sufficiently high sampling density over space, the spatial profile of the channel responses ( $g_i$ ) may be estimated by convolution (\*) of the detector impulse function with the stimulus waveform ( $f$ ):

$$g_i(x,y) = h_i(x,y)*f(x,y). \quad (\text{A10})$$

Combining Eqs. (A8), (A9) and (A10), the probability of seeing a stimulus may be written as:

$$P = 1 - (1 - \gamma) \exp\left(\sum_{i=1}^N \int \int_{-\infty}^{+\infty} |h_i(x,y)*f(x,y)|^\beta dx dy\right). \quad (\text{A11})$$

where  $N$  denotes the number of tuned channels and  $L$  is a constant.

At some fixed probability for stimulus detection we have:

$$\sum_{i=1}^N \int \int_{-\infty}^{+\infty} |h_i(x,y)*f(x,y)|^\beta dx dy = L. \quad (\text{A12})$$

It should be noted that Eq. (A12) describes probability summation across channels as well as across space.

## References

- Bijl, P., & Koenderink, J. J. (1993). Visibility of elliptical Gaussian blobs. *Vision Research*, 33, 243–255.
- Bracewell, R. N. (1978). *The Fourier Transform and its Applications*. New York: McGraw-Hill Book Company, Inc.
- Burgess, A., & Ghandeharian, H. (1984). Visual signal detection. I. Ability to use phase information. *Journal of the Optical Society of America A*, 54, 900–905.
- Burgess, A. (1999). The Rose model, revisited. *Journal of the Optical Society of America A*, 16, 633–646.
- Caelli, T., & Moraglia, G. (1987). Is pattern masking predicted by the cross-correlation between signal and mask? *Vision Research*, 27, 1319–1326.
- Campbell, F. W., & Kulikowski, J. J. (1966). Orientational selectivity of the human visual system. *Journal of Physiology London*, 187, 437–445.
- Campbell, F. W., & Robson, J. G. (1964). Application of Fourier analysis to the modulation response of the eye. *Journal of the Optical Society of America*, 54, 5871.
- Campbell, F. W., & Robson, J. G. (1968). Application of Fourier analysis to the visibility of gratings. *Journal of Physiology London*, 197, 551–566.
- Graham, N. (1989). *Visual Pattern Analysers*. Oxford: Clarendon Press.
- Graham, N., & Nachmias, J. (1971). Detection of grating patterns containing two spatial frequencies: a comparison of single-channel and multiple-channels models. *Vision Research*, 11, 251–259.

- Graham, N., & Robson, J. G. (1987). Summation of very close spatial frequencies: the importance of spatial frequency summation. *Vision Research*, 27, 1997–2007.
- Graham, N., Robson, J. G., & Nachmias, J. (1978). Grating summation in fovea and periphery. *Vision Research*, 18, 815–825.
- Green, D. B., & Swets, J. A. (1974). *Signal Detection Theory and Psychophysics*. New York: Wiley.
- Hall, J. L., & Sondhi, M. M. (1977). Detection threshold for a two-tone complex. *Journal of the Acoustical Society of America*, 62, 636–640.
- Hauske, G. (1988). The visual system as a spatial frequency matched filter. In H. Marko, G. Hauske, & A. Struppler, *Processing Structure for Perception and Action* (pp. 99–118). Weinheim, Germany: Verlag Chemie.
- Kersten, D. (1984). Spatial summation in visual noise. *Vision Research*, 24, 1977–1990.
- Koenderink, J. J., & van Doorn, A. J. (1978). Detectability of power fluctuations of temporal visual noise. *Vision Research*, 18, 191–195.
- Manahilov, V., & Simpson, W. (1999a). Energy model for contrast detection: spatiotemporal characteristics of threshold vision. *Biological Cybernetics*, 81, 61–71.
- Manahilov, V., Simpson, W., (1999b). A new look at spatial frequency and orientation selectivity of human pre-attentive vision. 3<sup>rd</sup> Annual Vision Research Conference, Abstract book, 106 (Abstract).
- Nachmias, J. (1981). On the psychometric function for contrast detection. Spatial-frequency channels in human vision. *Vision Research*, 21, 215–223.
- Pelli, G. D., & Zhang, L. (1991). Accurate control of contrast on microcomputer displays. *Vision Research*, 31, 1337–1350.
- Phillips, G. C., & Wilson, H. R. (1984). Orientation bandwidth of spatial mechanisms measuring by masking. *Journal of the Optical Society of America A*, 1, 226–232.
- Quick, R. F. Jr (1974). A vector-magnitude model of contrast detection. *Kybernetik*, 16, 65–67.
- Quick, F. R., Mullins, W. W., & Reichert, T. A. (1978). Spatial summation effects on two-component grating thresholds. *Journal of the Optical Society of America*, 68, 116–121.
- Rashbass, C. (1970). The visibility of transient changes of luminance. *Journal of Physiology (London)*, 210, 165–186.
- Ringach, D. L., Bredfeldt, C. E., Dorn, J. D., Spriggs, D., & Irazoqui-Pastor, P. (2000). Dynamics of spatial frequency selectivity in macaque primary visual cortex. *Investigative Ophthalmology and Visual Science*, 41(Suppl.), 333 (Abstract).
- Ringach, D. L., Hawken, M. J., & Shapley, R. (1997). Dynamics of orientation tuning in macaque primary visual cortex. *Nature*, 387, 281–284.
- Robson, J. G., & Graham, N. (1981). Probability summation and regional variation in contrast sensitivity across the visual field. *Vision Research*, 21, 409–418.
- Rovamo, J., Luntinen, O., & Näsänen, R. (1993). Modelling the dependence of contrast sensitivity on grating area and spatial frequency. *Vision Research*, 33, 2773–2788.
- Sach, M. B., Nachmias, J., & Robson, J. G. (1971). Spatial-frequency channels in human vision. *Journal of the Optical Society of America*, 61, 1176–1186.
- Simpson, A. W. (1994). Temporal summation of visual motion. *Vision Research*, 34, 2547–2559.
- Watson, A. B. (1979). Probability summation over time. *Vision Research*, 19, 515–522.
- Watson, A. B. (1982). Summation of grating patches indicates many types of detectors at one retinal location. *Vision Research*, 22, 17–25.

- Watson, A. B. (2000). Visual detection of spatial contrast patterns: evaluation of five simple models. *Optics Express*, 6, 12–33.
- Watson, A. B., & Nachmias, J. (1977). Patterns of temporal interactions in the detection of gratings. *Vision Research*, 17, 893–902.
- Watson, A. B., & Nachmias, J. (1980). Summation of asynchronous gratings. *Vision Research*, 20, 91–94.
- Wilson, H. R. (1980). Spatiotemporal characterization of a transient mechanism in the human visual system. *Vision Research*, 20, 443–452.